Annual Methodological Archive Research Review
http://amresearchreview.com/index.php/Journal/about
Volume 4, Issue 6 (2026)

Online ISSN 3007-3197
Print ISSN 3007-3189

http://amresearchreview.com/index.php/Journal/about

Comparative Physicochemical Characterisation, Antimicrobial, Anti-Inflammatory, and Analgesic Profiling of Silver Nanoparticles Biosynthesised from Sambucus wightiana Extract

Zafar ul Haq
Pharmacy Department, Hayatabad Medical Complex
Email: zafarpharmacist123@gmail.com

Dr. Waqar Ali (Corresponding Author)
Pharm D, M.Phil. Ph.D, Clinical Pharmacist, Department of Pharmacy, University of Peshawar, Pakistan Hayatabad Medical Complex, Peshawar, Pakistan
E-mail: aliwaqar241@gmail.com ORCID: 0000-0003-3186-6889

Dr. Abid Ali Ahmad
Assistant Professor, Department of Pharmacy, Qurtuba University of Science & Technology Peshawar Email: pharmacist.abid@gmail.com

Ziyad Khan
Pharmacist, Hayatabad Medical Complex, Peshawar, Pakistan
Email: ziyadrph@gmail.com

ABSTRACT

Background: Plant mediated green synthesized silver nanoparticles (AgNPs) are versatile nanomaterials as they possess inherent antimicrobial property with phytochemical bioactivity. Sambucus wightiana Wall. ex Wight & Arn. (Adoxaceae) is an ethnomedicinally important Himalayan shrub rich in flavonoids, tannins, and phenolic acids. Its potential as an AgNP precursor has not previously been reported in the literature.

Objective: To synthesize, fully characterize, and evaluate the antimicrobial, anti-inflammatory, and analgesic activities of AgNPs biosynthesized from the aqueous leaf extract of S. wightiana, and to contextualize the findings within the global literature on plant-mediated AgNPs.

Methods:

Silver nanoparticles (AgNPs) were biosynthesized by reacting 1 mM $AgNO_3$ with 10% (w/v) aqueous Sambucus wightiana extract under continuous stirring (350 rpm) at 37°C for 24 hours. The resulting AgNPs were characterized using UV–Vis, XRD, FTIR, SEM, TEM, EDS, DLS, and zeta potential analyses. Their antimicrobial activity was tested against nine bacterial and nine fungal strains using agar well diffusion and agar slant dilution methods, respectively, with the minimum inhibitory concentration (MIC) determined via broth microdilution. The anti-inflammatory and analgesic effects were evaluated in BALB/c mice using carrageenan-induced paw edema and hot plate tests after intraperitoneal injection of AgNPs at doses of 5, 10,

Annual Methodological Archive Research Review
http://amresearchreview.com/index.php/Journal/about
Volume 4, Issue 6 (2026)

Online ISSN 3007-3197
Print ISSN 3007-3189
http://amresearchreview.com/index.php/Journal/about

and 20 mg/kg. Results showed a color change to yellow-brown indicating AgNP formation, with UV-Vis revealing a peak at 423 nm. XRD confirmed a face-centered cubic (FCC) crystalline structure (JCPDS 04-0783), with the strongest (111) reflection at 38.2°. FTIR identified surface-capping phytochemicals with hydroxyl, C=C, C–N, and C=N groups. TEM showed mostly spherical, hexagonal, or rod-shaped particles, 12–30 nm in diameter. The Zeta potential of −24.5 mV indicated good colloidal stability. The AgNPs demonstrated strong antibacterial activity, notably against Escherichia coli (ZOI 28 mm; MIC 0.05 mg/mL) and Pseudomonas aeruginosa (ZOI 29 mm; MIC 0.02 mg/mL), along with antifungal activity against Fusarium solani (80% inhibition at 100 µg) and Aspergillus terreus (90% inhibition at 140 µg). At 20 mg/kg, AgNPs achieved 57.05% inhibition of carrageenan-induced paw edema after 5 hours ($P<0.001$) and 42.19% analgesic protection at 90 minutes ($P<0.001$)..

Conclusion: S. wightiana-mediated AgNPs exhibit broad-spectrum antimicrobial activity, anti-inflammatory effects, and analgesic properties, highlighting their potential as green-synthesized nanomaterials for pharmacological applications. Their antimicrobial potency exceeds that of AuNPs from the same source, attributed to silver ion-mediated disruption of bacterial membranes, enhanced by phytochemical synergy.

Keywords: Silver Nanoparticles; Green Synthesis; Sambucus Wightiana; Antimicrobial Activity; Anti-Inflammatory Activity; Analgesic Activity; X-Ray Diffraction; Zeta Potential

Introduction

Emerging resistance to antibiotics is a global problem and has been recognized as an emergency for the discovery of new compounds with a mechanism of action orthogonal to the existing antibiotic drugs [1]. The antimicrobial potential of silver nanoparticles (AgNPs) has been explored because the silver ion (Ag+) can interfere with several bacterial cellular components including respiratory chain enzymes, DNA replication machinery and phospholipids of the membrane, which makes it less likely to develop resistance compared to single-target antibiotics[2,3]. Considering the inherent toxicity of silver nanoparticles, coupled with the biological activity of surface bound phytochemical capping molecules, renders the plant mediated AgNPs as multi mechanism antibacterial system whose therapeutic potential is yet to be explored [4].

The green synthesis of AgNPs with plant extracts has become an attractive platform for the synthesis of biomedical-grade nanoparticles, as it is environmentally friendly, biocompatible and is also prepared in a single step at ambient temperature [5, 6]. Plant extracts contain phytochemicals which are mainly polyphenols, flavonoids, terpenoids, and organic acids that not only act as reducing agents ensuring $Ag^{+} \rightarrow Ag^{0}$ transformation, but also act as capping agents to stabilize the surface of the emerging nanoparticles and directly participate in the biological activities observed. [7]. Thus, careful selection of the plants will play a pivotal role in the physicochemical properties and bioactivity profile of the nanoparticles produced [8].

Sambucus wightiana Wall. ex Wight & Arn. The Himalayan elder (R. insulana L., family Adoxaceae) is a deciduous perennial shrub widely distributed in the

Annual Methodological Archive Research Review
http://amresearchreview.com/index.php/Journal/about
Volume 4, Issue 6 (2026)

Online ISSN 3007-3197
Print ISSN 3007-3189
http://amresearchreview.com/index.php/Journal/about

subHimalayan areas of Pakistan, India and Afghanistan. [9]. Ethnomedicinal data indicate its therapeutic application for inflammatory diseases, skin infections, gastrointestinal diseases, and febrile conditions. The phytochemical screening of the extract revealed the presence of alkaloids, glycosides, tannins, flavonoids and phenolic compounds as the pharmacologically active constituents, confirming the plants' medicinal properties [9, 10]. S. wightiana extract is a rich source of polyphenolic compounds, which are expected to have the ability to donate their electrons to metallic nanoparticles in view of the presence of electron-donating groups such as catechol and galloyl in its flavonoids [11].

The same plant was used in previous studies to successfully synthesize AuNPs which exhibited antimicrobial, anti-oxidative, anti-inflammatory and anti-analgesic activities. But the silver nanoparticles, although originating from the same botanical source, completely different on physicochemical and pharmacological properties. In particular, the AgNPs have a specific surface plasmon resonance profile, smaller particle sizes, different colloidal stability and higher antimicrobial activity as a consequence of disruption of the bacterial membrane mediated by Ag^{+} ions, which is not the case for gold systems. [2, 12].

For this reason, the study presents synthesize, fully characterize, and evaluate the antimicrobial, anti-inflammatory, and analgesic activities of AgNPs biosynthesized from the aqueous leaf extract of S. wightiana,

Materials and Methods

Plant Material and Extract Preparation

Entire S. wightiana plants were collected from the Kalam and Miandam localities of District Swat, Khyber Pakhtunkhwa, Pakistan. Botanical identity was confirmed at the Centre for Biodiversity and Taxonomy, University of Peshawar, where a voucher specimen was deposited for reference. The collected material was rinsed free of surface debris, air-dried in shade for four weeks, and reduced to a fine powder by mechanical grinding. To prepare the extract, 10 g of powdered plant material was added to 100 mL of deionized water and boiled with continuous agitation for 30 min, yielding a 10% (w/v) aqueous extract. After cooling to room temperature, the extract was passed through Whatman No. 1 filter paper to remove coarse particulates and further clarified by centrifugation (10,000 rpm, 10 min); the resulting supernatant was stored at 4°C until required for nanoparticle synthesis. Schematic workflow of the study methodology, from nanoparticle biosynthesis to biological assessment shown in figure 1.

Annual Methodological Archive Research Review
http://amresearchreview.com/index.php/Journal/about
Volume 4, Issue 6 (2026)

Online ISSN 3007-3197
Print ISSN 3007-3189

http://amresearchreview.com/index.php/Journal/about

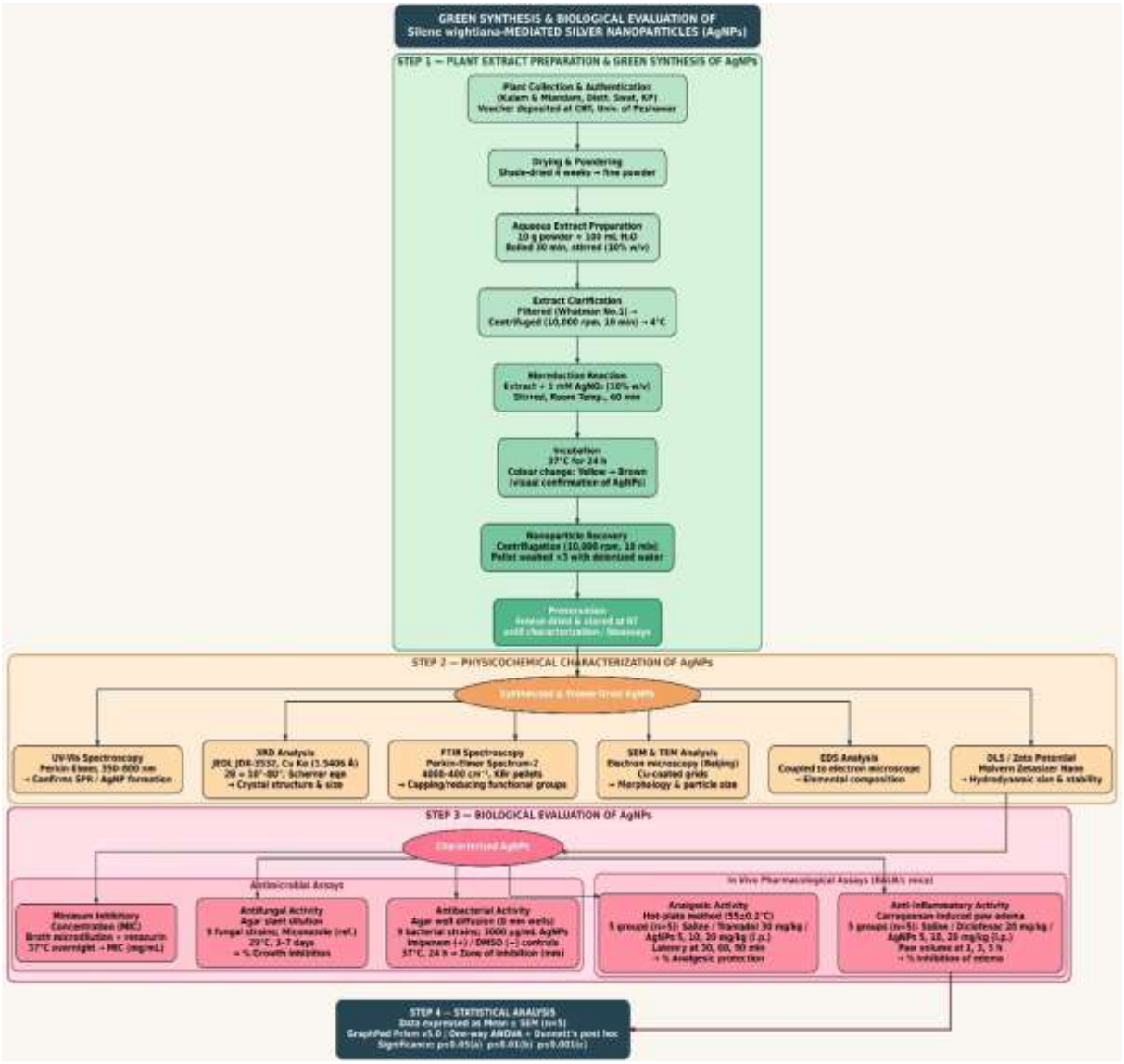

Figure 1: Schematic workflow of the study methodology, from nanoparticle biosynthesis to biological assessment

Results

Visual Observation and UV-Visible Spectrophotometry

As shown in Figure 2, AgNP formation was confirmed by the appearance of a yellow-brown color and a characteristic SPR peak at λmax = 423 nm in the UV–Vis spectrum [13, 14].

Annual Methodological Archive Research Review
http://amresearchreview.com/index.php/Journal/about
Volume 4, Issue 6 (2026)

Online ISSN 3007-3197
Print ISSN 3007-3189

http://amresearchreview.com/index.php/Journal/about

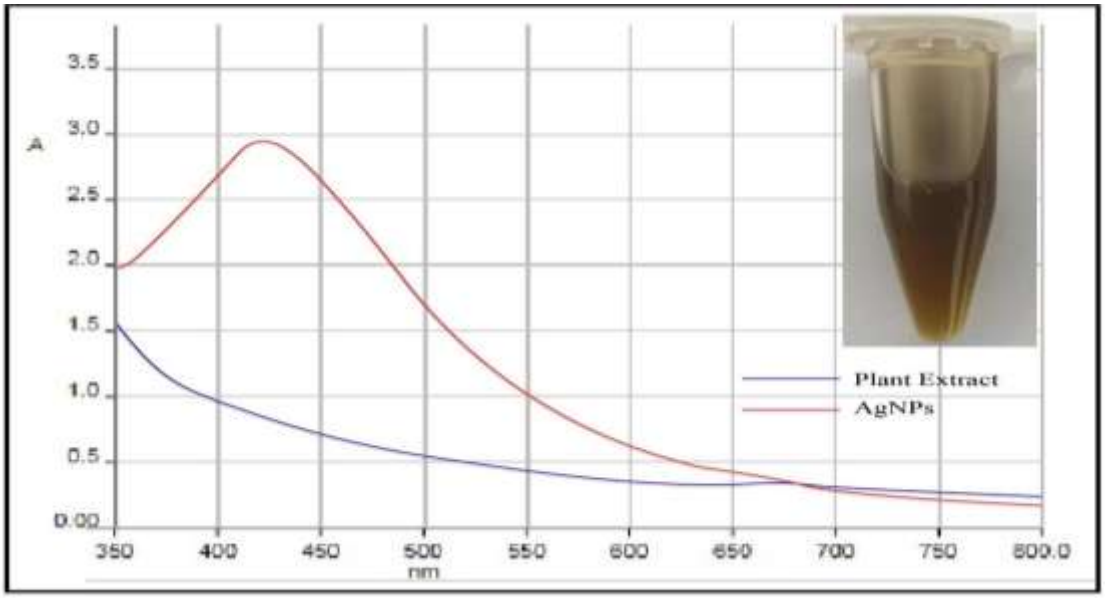

Figure 2: UV-Visible Absorption Spectrum of Sambucus wightiana-Mediated AgNPs

X-Ray Diffraction Analysis

As shown in Figure 3, XRD confirmed the crystalline FCC structure of AgNPs, with the dominant (111) peak indicating preferential crystal growth and no detectable impurity phases [15].

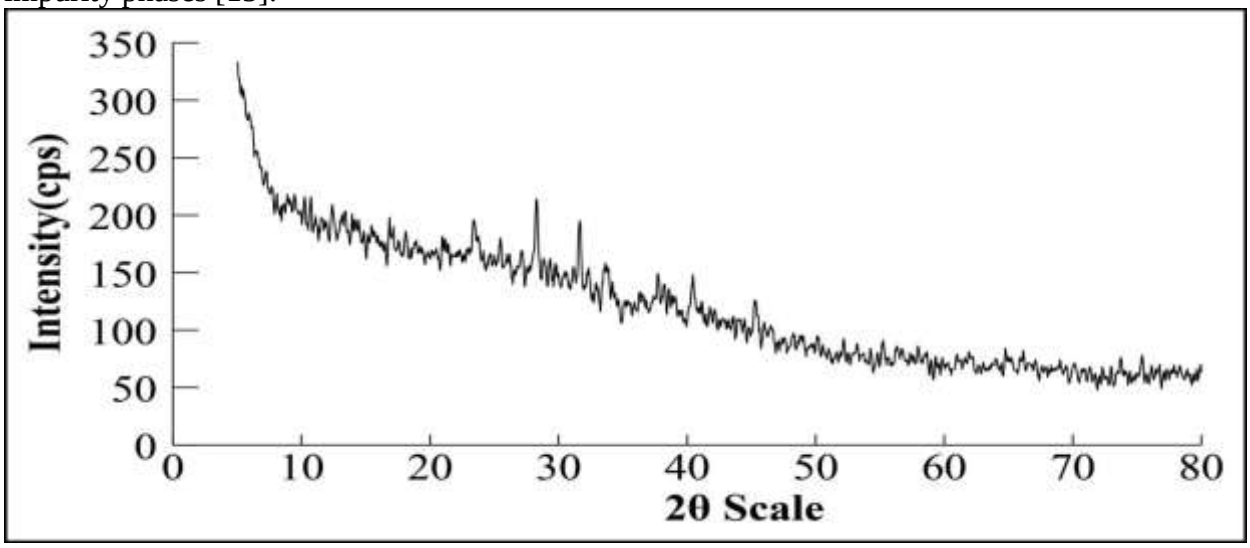

Figure 3: X-Ray Diffraction Pattern

FTIR Spectral Analysis

As shown in Figure 4, FTIR analysis confirmed that phenolic, flavonoid, and nitrogen-containing phytochemicals were involved in the reduction and stabilization of AgNPs, forming the capping layer on the nanoparticle surface [17].

Annual Methodological Archive Research Review
http://amresearchreview.com/index.php/Journal/about
Volume 4, Issue 6 (2026)

Online ISSN 3007-3197
Print ISSN 3007-3189
http://amresearchreview.com/index.php/Journal/about

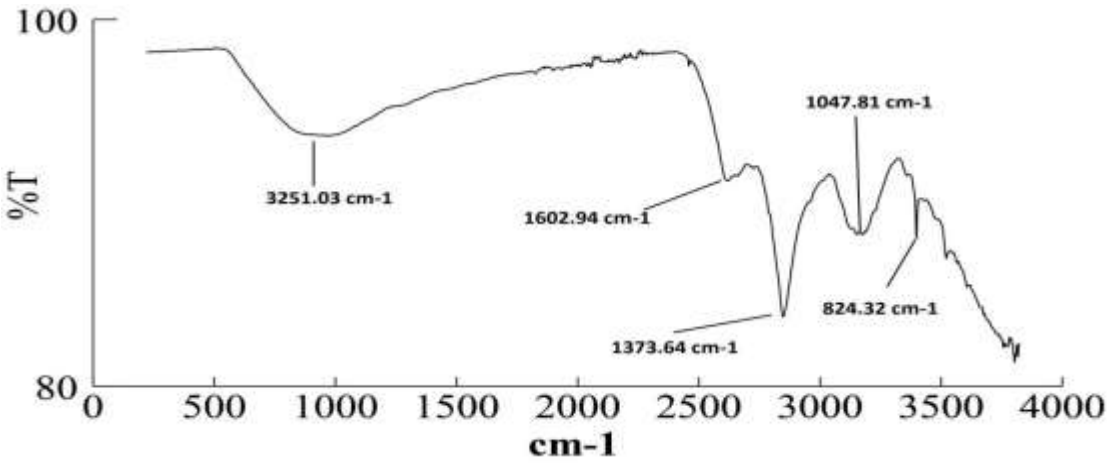

Figure 4: FTIR Spectrum

Scanning Electron Microscopy

The SEM analysis (Figure 5A–D) showed that the particles were mostly spherical, with some hexagonal, rod, and cubic shapes, which is indicative of the anisotropic nature of the biogenically synthesized particle. Moderate agglomeration was noted in the dried SEM sample, which is a typical artifact resulting from drying, and not indicative of the dispersed colloidal state [18].

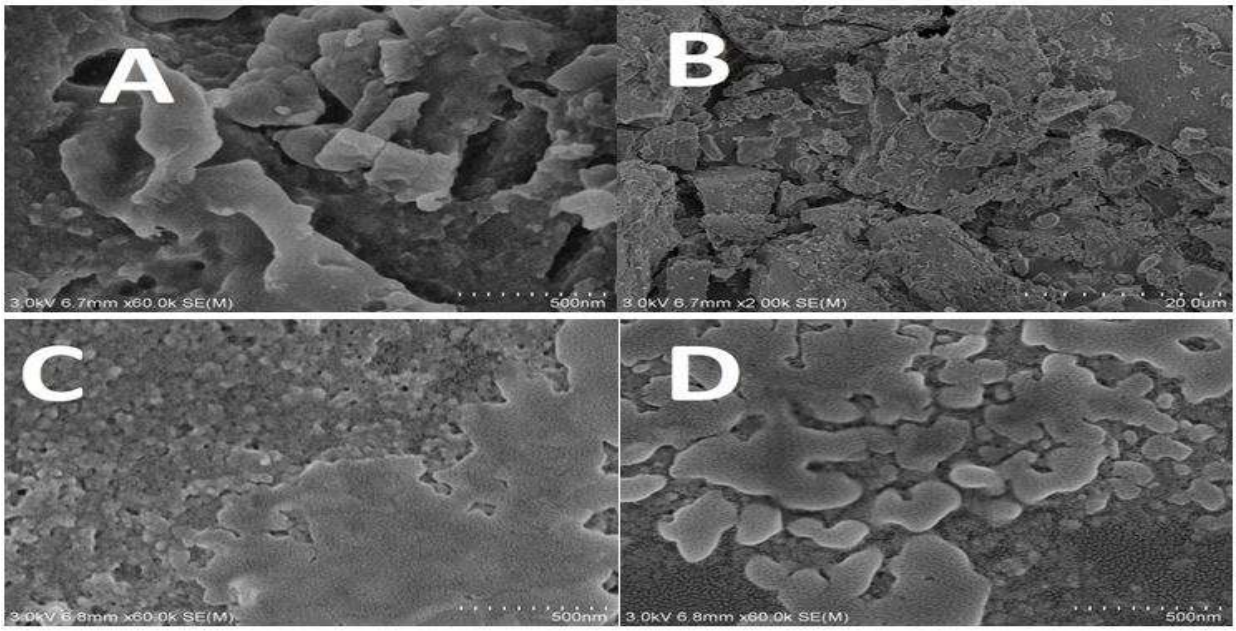

Figure 5(A-D): Scanning Electron Microscopy

Transmission Electron Microscopy and Particle Size Distribution

As shown in Figures 6A-D, TEM confirmed anisotropic AgNPs with sizes ranging from 12–30 nm (mean: 19.67 nm), a range considered optimal for enhanced antibacterial activity [19, 20].

Annual Methodological Archive Research Review
http://amresearchreview.com/index.php/Journal/about
Volume 4, Issue 6 (2026)

Online ISSN 3007-3197
Print ISSN 3007-3189

http://amresearchreview.com/index.php/Journal/about

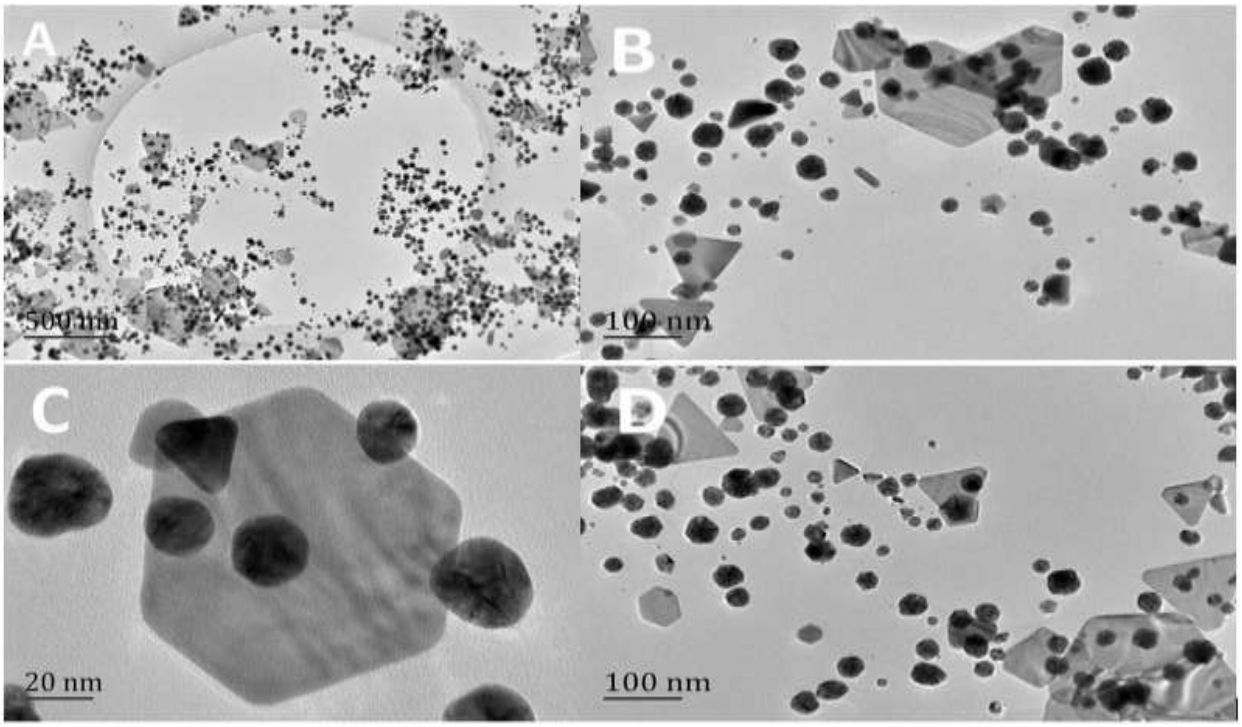

Figure 6: Transmission Electron Microscopy

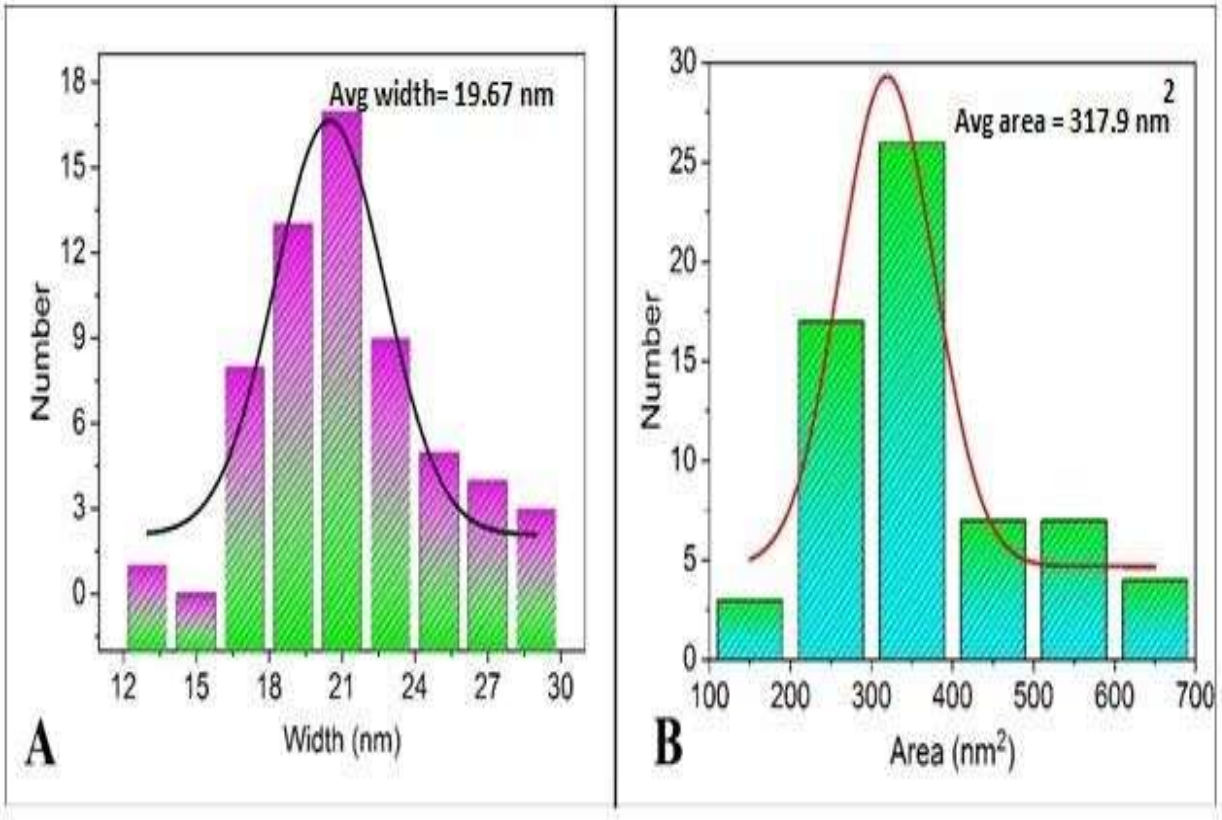

Figure 7: Particle Size Distribution Histogram and Zeta Potential

Annual Methodological Archive Research Review
http://amresearchreview.com/index.php/Journal/about
Volume 4, Issue 6 (2026)

Online ISSN 3007-3197
Print ISSN 3007-3189

http://amresearchreview.com/index.php/Journal/about

Energy Dispersive X-Ray Spectrometry and Zeta Potential

As shown in Figure 8, EDS confirmed the elemental purity of AgNPs, while a zeta potential of −24.5 mV and zeta size of 51 nm indicated good colloidal stability with a narrow size distribution [21, 22].

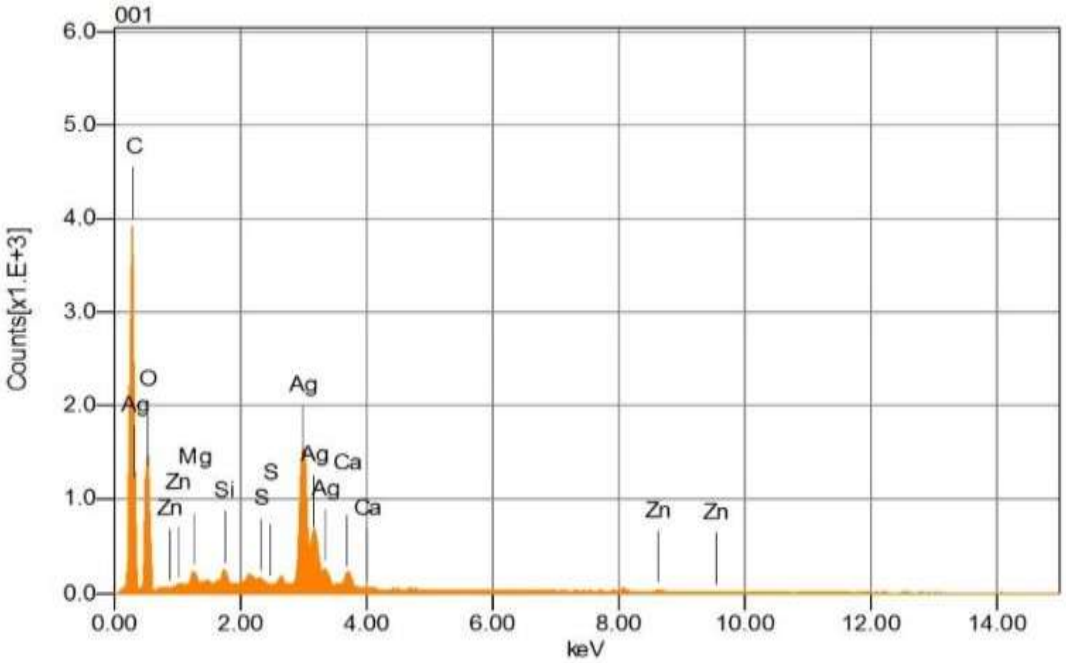

Figure 8: Energy Dispersive X-Ray Spectrometry

Antibacterial Activity

AgNPs exhibited broad-spectrum antibacterial activity against all nine bacterial strains. Among Gram-negative species, E. coli was most sensitive (ZOI 28 mm; MIC 0.05 mg/mL), followed by Pseudomonas aeruginosa (ZOI 29 mm; MIC 0.02 mg/mL), Salmonella enteritidis (ZOI 24 mm; MIC 0.01 mg/mL), Salmonella typhi (ZOI 18 mm; MIC 0.15 mg/mL), Klebsiella pneumoniae, and Shigella flexneri. Among Gram-positive species, Staphylococcus epidermidis was inhibited (ZOI 27 mm; MIC 0.01 mg/mL), and Bacillus subtilis was also susceptible. The plant extract alone showed measurable but lower antibacterial activity, whereas the nanoparticle formulation produced larger ZOIs and lower MICs (Table 1), confirming nanoparticle-specific efficacy beyond simple phytochemical effects. AgNPs consistently outperformed AuNPs from the same botanical source across all bacterial strains, consistent with the established superior intrinsic antimicrobial potency of silver over gold at equivalent concentrations [12].

Antifungal Activity

Antifungal activity was selective. Fusarium solani was the most sensitive fungal species with 80% inhibition at 100 µg (MIC 0.01 mg/mL); Aspergillus terreus showed 90% inhibition at 140 µg. Microsporum canis was inhibited by 50% (MIC 0.02 mg/mL), and Alternaria alternata by 70% (MIC 0.15 mg/mL). Aspergillus niger showed 60% inhibition at 210 µg. No inhibitory activity was detected against

Annual Methodological Archive Research Review
http://amresearchreview.com/index.php/Journal/about
Volume 4, Issue 6 (2026)

Online ISSN 3007-3197
Print ISSN 3007-3189

http://amresearchreview.com/index.php/Journal/about

Aspergillus flavus, Trichophyton longifusis, or Candida glabrata within the tested concentration range, while Candida albicans showed limited inhibition. AgNPs demonstrated comparable or superior activity to AuNPs from the same source, particularly against Fusarium solani and Alternaria alternata (Table 2).

In Vivo Anti-Inflammatory Activity

AgNPs produced dose-dependent suppression of carrageenan-induced hind paw edema (Table 3). At 5 mg/kg, inhibition was less significant ($p \leq 0.05$) at 1–3 hours, increasing to significant ($p \leq 0.01$) at 5 hours (35.71% inhibition). At 10 mg/kg, inhibition progressed from significant ($p \leq 0.01$) at 1 hour (34.45%) to highly significant ($p \leq 0.001$) at 5 hours (46.37%). At 20 mg/kg, inhibition reached 39.01% at 1 hour ($p \leq 0.001$), increasing progressively to 57.05% at 5 hours ($p \leq 0.001$). The standard drug Diclofenac sodium (20 mg/kg) produced 54.38% and 72.04% inhibition at 1 and 5 hours, respectively. The progressive increase in anti-inflammatory activity over 5 hours is consistent with a sustained-release mechanism of phytochemical from the nanoparticle surface, consistent with previous reports on polyphenol-capped nanoparticles [23].

In Vivo Analgesic Activity (Hot-Plate Method)

AgNPs produced a statistically significant, dose-dependent elevation in thermal pain thresholds (Table 4). At 5 mg/kg, no significant activity was observed at 30 and 90 minutes, with less significant activity ($p \leq 0.05$) at 60 minutes (21.06% protection). At 10 mg/kg, a significant analgesic effect ($p \leq 0.01$) was observed at 30 and 60 minutes, with a less significant effect ($p \leq 0.05$) persisting at 90 minutes. At 20 mg/kg, highly significant analgesic protection ($p \leq 0.001$) was demonstrated throughout the 90-minute observation period (33.51%, 53.24%, and 42.19% protection at 30, 60, and 90 minutes, respectively), with performance approaching that of the positive control Tramadol (30 mg/kg; 54.47%, 59.71%, 59.42% protection). The analgesic profile is consistent with both peripheral (COX inhibition via surface-bound flavonoids and phenolic acids) and central (opioid pathway modulation) mechanisms [24].

Table 1: Antibacterial Activity of AgNPs from Sambucus wightiana: ZOIand MIC

Microorganism	Plant extract ZOI (mm)	Plant extract MIC (mg/mL)	AgNPs ZOI (mm)	AgNPs MIC (mg/mL)	AuNPs ZOI (mm)[a]	Standard (Imipenem) ZOI (mm)
Escherichia coli	14	0.69	28	0.05	25	33
Pseudomonas aeruginosa	10	0.78	29	0.02	NI	32
Salmonella enteritidis	14	0.66	24	0.01	18	31
Salmonella typhi	10	0.81	18	0.15	15	33
Klebsiella pneumoniae	NI	ND	ND	ND	NI	16
Shigella flexneri	NI	ND	ND	ND	NI	35

Annual Methodological Archive Research Review
http://amresearchreview.com/index.php/Journal/about
Volume 4, Issue 6 (2026)

Online ISSN 3007-3197
Print ISSN 3007-3189

http://amresearchreview.com/index.php/Journal/about

Staphylococcus aureus	NI	ND	ND	ND	NI	30
Bacillus subtilis	NI	ND	*	ND	NI	36
Staphylococcus epidermidis	15	0.35	27	0.01	23	29

Table 2: Antifungal Activity of Sambucus wightiana AgNPs: Percentage Inhibition (% I) and MIC Against Selected Fungal Strains

Microorganism	Plant extract % I	Plant extract MIC (mg/mL)	AgNPs % I	AgNPs conc. (µg)	AgNPs MIC (mg/mL)	AuNPs % I[a]	Standard (Miconazole) % I
Alternaria alternata	40%	0.61	70%	140	0.15	40%	100%
Aspergillus flavus	NI	—	NI	—	—	NI	100%
Aspergillus niger	40%	0.75	60%	210	0.20	30%	100%
Aspergillus terreus	30%	0.65	90%	140	0.81	50%	100%
Candida albicans	NI	—	30%	910	—	NI	100%
Candida glabrata	NI	—	30%	—	0.88	NI	100%
Fusarium solani	30%	0.80	80%	100	0.01	90%	100%
Microsporum canis	40%	0.45	50%	210	0.02	80%	100%
Trichophyton longifusis	NI	—	NI	—	—	NI	100%

Table 3: Anti-Inflammatory Activity of Sambucus wightiana AgNPs: Effect on Carrageenan-Induced Hind Paw Oedema in BALB/c Mice

Tested Group	Dose (mg/kg)	Basal Volume (mL)	Mean Paw Volume at 1 h (mL) [%inhibition]	Mean Paw Volume at 3 h (mL) [%inhibition]	Mean Paw Volume at 5 h (mL) [%inhibition]	Statistical significance at 5 h
Negative Control	—	0.091 ± 0.023	0.249 ± 0.002	0.251 ± 0.001	0.259 ± 0.002	—
AgNPs	5	0.150 ± 0.021	0.230 ± 0.005 [26.76%]	0.190 ± 0.005 [31.82%]	0.189 ± 0.005 [35.71%]	p≤0.01 (b)
AgNPs	10	0.110 ± 0.021	0.192 ± 0.006 [34.45%]	0.178 ± 0.006 [39.93%]	0.164 ± 0.008 [46.37%]	p≤0.001 (c)
AgNPs	20	0.100 ± 0.021	0.172 ± 0.007 [39.01%]	0.163 ± 0.005 [47.17%]	0.148 ± 0.052 [57.05%]	p≤0.001 (c)
Diclofenac Na	20	0.110 ±	0.147 ± 0.005	0.128 ± 0.026	0.125 ± 0.003	p≤0.001 (c)

Annual Methodological Archive Research Review
http://amresearchreview.com/index.php/Journal/about
Volume 4, Issue 6 (2026)

Online ISSN 3007-3197
Print ISSN 3007-3189

http://amresearchreview.com/index.php/Journal/about

		0.022	[54.38%]	[62.36%]	[72.04%]	

Table 4: Analgesic Activity of Sambucus wightiana AgNPs: Thermal Hot-Plate Latency (seconds) in Mice

Tested Group	Dose (mg/kg)	Mean Latency at 30 min (s) [%protection]	Mean Latency at 60 min (s) [%protection]	Mean Latency at 90 min (s) [%protection]	Statistical significance at 90 min
Negative Control	—	9.68 ± 0.24	10.74 ± 0.36	11.09 ± 0.42	—
AgNPs	5	13.12 ± 0.56 [16.13%]	14.99 ± 0.46 [21.06%][a]	13.94 ± 0.52 [14.26%]	NS
AgNPs	10	14.47 ± 0.42 [22.46%][b]	17.43 ± 0.52 [33.14%][b]	15.39 ± 0.52 [22.55%][a]	p≤0.05 (a)
AgNPs	20	16.86 ± 0.29 [33.51%][c]	21.74 ± 0.68 [53.24%][c]	19.30 ± 0.58 [42.19%][c]	p≤0.001 (c)
Tramadol (standard)	30	21.32 ± 0.79 [54.47%][c]	22.88 ± 0.50 [59.71%][c]	22.89 ± 0.73 [59.42%][c]	p≤0.001 (c)

Discussion

This study reports the physicochemical characteristics and biological evaluation of AgNPs synthesized from Sambucus wightiana leaf extract. The rapid color change (colorless to yellow-brown) upon mixing the S. wightiana extract with AgNO3 reflects the kinetics of polyphenol-mediated Ag^{+} reduction. The phenolic hydroxyl groups of flavonoids and phenolic acids identified by FTIR in the S. wightiana extract act as electron donors, oxidizing to ortho-quinone forms while reducing Ag^{+} to Ag^{0} through a stepwise single-electron transfer mechanism [7].

The difference in the O–H stretching frequency of the AgNP FTIR spectrum with the O–H stretching frequency of the free extract is indicative of the fact that the –OH groups in the extract are directly coordinated to the Ag surface and thus act as capping stabilizing ligands [17]. The Zeta Potential value of 24.5 mV is slightly below the critical threshold of 30 mV, suggesting good colloidal stability [22] and the identification of multiple organic functional groups on the surface of the nanoparticles (C=C, C–N, C=N, N–O bands) confirms the presence of a multi-component capping layer, in line with the multi-component phytochemical complexity of the extract from S. wightiana.

Completeness of the reduction of the silver precursor was confirmed by the XRD pattern, which showed no peak corresponding to Ag2O and AgCl, contaminant of the silver. In many previous studies of AgNPs produced by plants, preferential growth along the [111] direction has been observed and linked to the preferential binding of phytochemicals to the high energy (111) faces of the AgNPs, which impedes crystal growth along these faces [15]. The range of particle size (12–30 nm) in the TEM is comparable to that of other medicinal plants reported to produce AgNPs, such as

Annual Methodological Archive Research Review
http://amresearchreview.com/index.php/Journal/about
Volume 4, Issue 6 (2026)

Online ISSN 3007-3197
Print ISSN 3007-3189
http://amresearchreview.com/index.php/Journal/about

Camellia sinensis (10–25 nm) [25], Azadirachta indica (15–30 nm) [26] and Curcuma longa (15–35 nm) [27].

The significantly higher antimicrobial activity of S. wightiana AgNPs over the AuNPs as reported in the previous article [26] is due to the difference in the antimicrobial mechanism of silver nanoparticles. The main mechanism involves the release of Ag^+ ions from the surface of the nanoparticle that disrupts several cellular targets of bacteria: the inner membrane, the respiratory chain, and the replication of DNA, by intercalating between the chains of phospholipid fatty acids, by inhibiting NADH dehydrogenase and the electron transport chain, and by binding directly to the Ag^+–DNA phosphate complex, respectively [2, 3]. The complexity of mechanisms means that resistance is much less likely to develop to this type of antibiotic than to single target antibiotics. The antibacterial activity of AuNPs, however, is mainly due to the intrinsic antibacterial activity of the nanoparticles themselves, which act by membrane disruption, without the release of ions, causing a categorically lower intrinsic antibacterial activity [12].

The counter-intuitive observation of the observed sensitivity of Gram-negative bacteria rather than Gram-positive is explained by the membrane architecture of Gram-negative bacteria: the outer membrane, which is rich in LPS, electrostatically attracts the negatively charged AgNPs (zeta potential = −24.5 mV), which can overcome the electrostatic barrier with positive-charge mediated LPS interaction [3,28]. In addition, the LPS lipid A component of LPS provides insertion sites for membrane disruption by nanoparticles that are not available in Gram-positive membranes. Furthermore, the intrinsic antibacterial property of phytochemicals used as capping agents has been independently confirmed in the S. wightiana extract, thus adding additional synergistic contribution to the antimicrobial activity achieved by using chemically synthesized AgNPs that are stabilized by an inert polymer [9].

The antibacterial activity of S. wightiana AgNPs are comparable to Ocimum tenuiflorum AgNPs (MIC 0.025–0.10 mg/mL) [29] and Aloe vera AgNPs (MIC 0.05–0.20 mg/mL) [30] and better than Moringa oleifera AgNPs (MIC 0.10–0.50 mg/mL) [31] as compared to the global literature.

The anti-inflammatory activity of AgNPs is attributed to the core of the AgNPs and the phytochemicals bound to the surface of the nanoparticles, which have different modes of action. Mechanistic studies on silver nanoparticles from comparable plant systems have demonstrated downregulation of pro-inflammatory markers (TNF-α, IL-6, IL-1β) and inhibition of NF-κB signaling pathways, with nanoparticle sizes of 10–30 nm (consistent with S. wightiana AgNPs) showing optimal cellular uptake by macrophages and dendritic cells [32]. The surface-bound flavonoids and phenolic acids provide an additional anti-inflammatory mechanism by directly inhibiting cyclooxygenase (COX-1/COX-2) enzymes, as documented for quercetin, kaempferol, and chlorogenic acid, phytochemicals reported in Sambucus species [9,33].

The percentage inhibition at 20 mg/kg after 5 hours (57.05%) approaches but does not reach that of Diclofenac sodium (72.04%), a common finding in plant-derived nanoparticle anti-inflammatory studies and may reflect the lower intrinsic potency of phytochemical mechanisms relative to direct COX inhibitors at equivalent doses [23]. Compared with S. wightiana AuNPs reported in the published article (57.66% inhibition at 20 mg/kg after 5 hours), the AgNPs (57.05%) showed near-identical anti-

Annual Methodological Archive Research Review
http://amresearchreview.com/index.php/Journal/about
Volume 4, Issue 6 (2026)

Online ISSN 3007-3197
Print ISSN 3007-3189
http://amresearchreview.com/index.php/Journal/about

inflammatory efficacy, suggesting the anti-inflammatory effect is primarily phytochemical in origin, attributable to surface-capping flavonoids and phenolic acids from S. wightiana, with minimal contribution from the metallic core.

The thermal hot-plate method primarily evaluates supraspinal opioidergic analgesic mechanisms (reflecting central analgesic activity), whereas chemically induced pain models (e.g., acetic acid writhing) predominantly assess peripheral sensitization [34]. The significant analgesic effect of S. wightiana AgNPs at 20 mg/kg ($p \leq 0.001$ at all-time points), approaching Tramadol performance, suggests a central component in the analgesic mechanism. This is consistent with proposed mechanisms for nanomaterial-mediated analgesia involving nanoparticle-mediated modulation of cyclic AMP (cAMP) pathways and inhibition of tetrodotoxin-resistant (TTX-r) sodium channels in nociceptive neurons [35]. The peripheral COX-inhibitory contribution of surface flavonoids provides an additional analgesic mechanism, complementary to the central effect.

The analgesic performance of AgNPs (42.19% protection at 90 min, 20 mg/kg) was lower than that of AuNPs reported in the published article (46.48% protection at 90 min, 20 mg/kg) [26]. This difference may reflect differential CNS penetration between the two nanoparticle types, attributable to their distinct surface charge profiles and size distributions, though this hypothesis requires dedicated pharmacokinetic investigation.

Strengths and Limitations

The study exhibits noteworthy methodological and scientific merits, fully characterising the synthesised materials by UV-Vis, XRD, FTIR and other techniques to allow for clear distinction from other nanoparticles. It covers a broad spectrum of biological activities, which are more comprehensive than studies with limited number of endpoints. A novel, intra-study comparison between AgNPs and AuNPs reveals the importance of the identity of the metallic core on the differences in activity observed. The disadvantages are that AgNPs are not antioxidant, zeta potential results suggest potential aggregation, there are no in vitro mechanistic studies, and there are only a few in vivo group sizes, no pharmacokinetic data and inadequate characterization of capping agents. Future studies should be aimed at filling these gaps for a full understanding of the bioactivities of these materials.

Future Perspectives

Future research directions are identified such as HPLC-MS characterization of phytochemicals in S. wightiana extract for identifying reducing agents, in-vitro cytotoxicity study against cancer and normal cell lines for identification of therapeutic window, and antioxidant activity evaluations being immediate. Future aims encompass optimizing the synthesis via response surface methodology (RSM), understanding the role of the components of the nanoparticles in mechanistic studies, performing pharmacokinetic studies in mice and studying the anticancer activity of Ag nanoparticles and the development of nanoformulations for topical antimicrobial application. In total, the current study and other previously published work of AuNPs paved the way for the study of the bimetallic Ag-Au nanoparticles, which have the potential for synergistic biological activity [36].

Online ISSN 3007-3197
Print ISSN 3007-3189
http://amresearchreview.com/index.php/Journal/about

Conclusion

This study demonstrated the successful green synthesis of silver nanoparticles (AgNPs) using *Sambucus wightiana* leaf extract. The synthesized AgNPs were predominantly spherical, measuring 12–30 nm, and exhibited good colloidal stability. They showed potent antibacterial activity, particularly against Gram-negative pathogens including *E. coli*, *P. aeruginosa*, and *Salmonella* spp. (MIC as low as 0.01 mg/mL), along with notable antifungal effects against *Fusarium solani* and *Aspergillus terreus*. In addition, the AgNPs exhibited significant anti-inflammatory and analgesic activities in murine models. These findings highlight the potential of *S. wightiana*-derived AgNPs as multifunctional nanomaterials with promising therapeutic applications, particularly in combating antimicrobial resistance.

References

[1] Antimicrobial Resistance Collaborators. Global burden of bacterial antimicrobial resistance in 2019: a systematic analysis. Lancet. 2022; 399(10325):629–655.
[2] Slavin YN, Asnis J, Häfeli UO, Bach H. Metal nanoparticles: understanding the mechanisms behind antibacterial activity. J Nanobiotechnology. 2017;15(1):65.
[3] Marambio-Jones C, Hoek EMV. A review of the antibacterial effects of silver nanomaterials and potential implications for human health and the environment. J Nanopart Res. 2010;12:1531–1551.
[4] Khandel P, Yadaw RK, Soni DK, Kanwar L, Shahi SK. Biogenesis of metal nanoparticles and their pharmacological applications: present status and application prospects. J Nanostructure Chem. 2018;8:217–254.
[5] Iravani S. Green synthesis of metal nanoparticles using plants. Green Chem. 2011;13:2638–2650.
[6] Narayanan KB, Sakthivel N. Green synthesis of biogenic metal nanoparticles by terrestrial and aquatic phototrophic and heterotrophic eukaryotes and biocompatible agents. Adv Colloid Interface Sci. 2011;169(2):59–79.
[7] Mittal AK, Chisti Y, Banerjee UC. Synthesis of metallic nanoparticles using plant extracts. Biotechnol Adv. 2013;31(2):346–356.
[8] Ahmed S, Annu, Ikram S, Yudha S. Biosynthesis of gold nanoparticles: a green approach. J Photochem Photobiol B. 2016;161:141–153.
[9] Khandel P, Shahi SK. Mycogenic nanoparticles and their bio-prospecting for antimicrobial applications: a systematic review. J Nanostructure Chem. 2018;8:369–391.
[10] Daniel MC, Astruc D. Gold nanoparticles: assembly, supramolecular chemistry, quantum-size-related properties, and applications toward biology, catalysis, and nanotechnology. Chem Rev. 2004;104(1):293–346.
[11] Makarov VV, Love AJ, Sinitsyna OV, Makarova SS, Yaminsky IV, Taliansky ME, Kalinina NO. Green nanotechnologies: synthesis of metal nanoparticles using plants. Acta Naturae. 2014;6(1):35–44.
[12] Shamaila S, Zafar N, Riaz S, Sharif R, Nazir J, Naseem S. Gold nanoparticles: an efficient antimicrobial agent against enteric bacterial human pathogen. Nanomaterials. 2016;6(4):71.
[13] Moulton MC, Braydich-Stolle LK, Nadagouda MN, Kunzelman S, Hussain SM,

Online ISSN 3007-3197
Print ISSN 3007-3189

Varma RS. Synthesis, characterization and biocompatibility of "green" synthesized silver nanoparticles using tea polyphenols. Nanoscale. 2010;2:763–770.

[14] Milosavljevic V, et al. Alternative synthesis route of biocompatible polyvinylpyrrolidone nanoparticles and their effect on pathogenic microorganisms. Mol Pharm. 2017;14(1):221–233.

[15] Zhou Y, Lin W, Huang J, Wang W, Gao Y, Lin LYG, Li Q, Lin L, Du M. Biosynthesis of gold nanoparticles by foliar broths: roles of biocompounds and other attributes of the extracts. Nanoscale Res Lett. 2010;5:1351–1359.

[16] Konwarh R, Gogoi B, Philip R, Laskar MA, Karak N. Biomimetic preparation of polymer-supported free radical scavenging, cytocompatible and antimicrobial "green" silver nanoparticles using aqueous extract of Citrus sinensis peel. Colloids Surf B. 2011;84:338–345.

[17] Wang W, Chen Q, Jiang C, Yang D, Liu X, Xu S. One-step synthesis of biocompatible gold nanoparticles using gallic acid in the presence of poly(N-vinyl-2-pyrrolidone). Colloids Surf A. 2007;301:73–79.

[18] Njagi EC, Huang H, Stafford L, Genuino H, Galindo HM, Collins JB, Hoag GE, Suib SL. Biosynthesis of iron and silver nanoparticles at room temperature using aqueous sorghum bran extracts. Langmuir. 2011;27(1):264–271.

[19] Sathishkumar M, Sneha K, Won SW, Cho CW, Kim S, Yun YS. Cinnamon zeylanicum bark extract and powder mediated green synthesis of nano-crystalline silver particles and its bactericidal activity. Colloids Surf B. 2009;73:332–338.

[20] Rai MK, Deshmukh SD, Ingle AP, Gade AK. Silver nanoparticles: the powerful nanoweapon against multidrug-resistant bacteria. J Appl Microbiol. 2012;112(5):841–852.

[21] Seralathan J, Stevenson P, Subramaniam S, Raghavan R, Pemaiah B, Sivasubramanian A, Veerappan A. Spectroscopy investigation on chemo-catalytic, free radical scavenging and bactericidal properties of biogenic silver nanoparticles synthesized using Salicornia brachiata aqueous extract. Spectrochim Acta A. 2014;118:349–355.

[22] Tamuly C, Hazarika M, Bordoloi M, Bhattacharyya PK, Kar R. Biosynthesis of Ag nanoparticles using pedicellamide and its photocatalytic activity: an eco-friendly approach. Spectrochim Acta A. 2014;132:687–691.

[23] Ahmad A, et al. Synthesis of phytochemicals-stabilized gold nanoparticles and their biological activities against bacteria and Leishmania. Microbial Pathog. 2017;110:304–312.

[24] Fawad K, Islam NU, Subhan F, Shahid M, Ali G, Rahman FU, Mahmood W, Ahmad N. Novel hydroquinone derivatives alleviate algesia, inflammation and pyrexia in the absence of gastric ulcerogenicity. Trop J Pharm Res. 2018;17:53–63.

[25] Niraimathi KL, Sudha V, Lavanya R, Brindha P. Biosynthesis of silver nanoparticles using Alternanthera sessilis (Linn.) extract and their antimicrobial, antioxidant activities. Colloids Surf B. 2013;102:288–291.

[26] Khuda F, Iqbal Z, Khan A, Nasir F. Antimicrobial and anti-inflammatory activities of leaf extract of Valeriana wallichii DC. Pak J Pharm Sci.

Online ISSN 3007-3197
Print ISSN 3007-3189

2012;25(4):715–719.

[27] Shankar SS, Ahmad A, Pasricha R, Sastry M. Bioreduction of chloroaurate ions by geranium leaves and its endophytic fungus yields gold nanoparticles of different shapes. J Mater Chem. 2003;13:1822–1826.

[28] Rao ML, Savithramma N. Biological synthesis of silver nanoparticles using Svensonia hyderabadensis leaf extract and evaluation of their antimicrobial efficacy. J Pharm Sci Res. 2011;3(3):1117–1121.

[29] Jeyaraj M, Rajesh M, Arun R, Mubarak Ali D, Sathishkumar G, Sivanandhan G, et al. An investigation on the cytotoxicity and caspase-mediated apoptotic effect of biologically synthesized silver nanoparticles using Podophyllum hexandrum on human cervical carcinoma cells. Colloids Surf B. 2013;102:708–717.

[30] Haverkamp RG, Marshall AT. The mechanism of metal nanoparticle formation in plants: limits on accumulation. J Nanopart Res. 2009;11:1453–1463.

[31] Khalil AT, Ovais M, Ullah I, Ali M, Shinwari ZK. Physical properties, biological applications and biocompatibility studies on biosynthesized single phase cobalt oxide (Co_3O_4) nanoparticles via Sageretia thea (Osbeck.). Arab J Chem. 2020; 13(1):606–619.

[32] Patra CR, Bhattacharya R, Mukhopadhyay D, Mukherjee P. Fabrication of gold nanoparticles for targeted therapy in pancreatic cancer. Adv Drug Deliv Rev. 2010; 62:346–361.

[33] Durán N, Marcato PD, Durán M, Yadav A, Gade A, Rai M. Mechanistic aspects in the biogenic synthesis of extracellular metal nanoparticles by peptides, bacteria, fungi, and plants. Appl Microbiol Biotechnol. 2011;90:1609–1624.

[34] Thangaraj M, Gengan RM, Ranjan B, Muthusamy R. Synthesis, molecular docking, antimicrobial, antioxidant and toxicity assessment of quinoline peptides. J Photochem Photobiol B. 2018;178:287–295.

[35] Tiede K, Boxall ABA, Tear SP, Lewis J, David H, Hassellov M. Detection and characterization of engineered nanoparticles in food and the environment. Food Addit Contam A. 2008;25(7):795–821.

[36] Makarov VV, Makarova SS, Love AJ, Sinitsyna OV, Dudnik AO, Yaminsky IV, Taliansky ME, Kalinina NO. Biosynthesis of stable iron oxide nanoparticles in aqueous extracts of Hordeum vulgare and Rumex acetosa plants. Langmuir. 2014; 30:5982–5988.